Applied Thermal Engineering 116 (2017) 244–252

Contents lists available at ScienceDirect

Applied Thermal Engineering

journal homepage: www.elsevier.com/locate/apthermeng

Research Paper

Combustion properties of coal gangue using thermogravimetry–Fourier transform infrared spectroscopy

Jun Deng [a,b], Bei Li [a,b], Yang Xiao [a,b], Li Ma [a,b], Cai-Ping Wang [a,b], Bin Lai-wang [c], Chi-Min Shu [c,*]

[a] School of Safety Science and Engineering, Xi'an University of Science and Technology, Xi'an 710054, China
[b] Key Laboratory of Western Mine Exploration and Hazard Prevention, Xi'an University of Science and Technology, Ministry of Education, Xi'an 710054, China
[c] Department of Safety, Health, and Environmental Engineering, National Yunlin University of Science and Technology (YunTech), Douliou 64002, Yunlin, Taiwan, ROC

HIGHLIGHTS

- Five characteristic temperatures and mass losses of CG were investigated.
- Properties of the spontaneous combustion of CG were revealed through TG.
- Functional groups variation of CG was examining by FTIR under air atmosphere.
- S_n, D_i, and D_h values were calculated based on combustion performance method.
- S_n value increased with an increase in the $V_{ad} + FC_{ad}/A_{ad}$ value.

ARTICLE INFO

Article history:
Received 3 October 2016
Accepted 24 January 2017
Available online 27 January 2017

Keywords:
Gangue dump
Thermogravimetry
Combustion performance indices
Spontaneous combustion process
De-volatilization rate

ABSTRACT

This study investigated the combustion properties of coal gangue (CG) from the Gongwusu coal mine in northern China. Three CG samples collected from various parts of the spontaneous combustion gangue dump were evaluated using a proximate analyzer, thermogravimetry, and Fourier transform infrared spectroscopy. The results revealed that the total mass losses of the three samples were 15.5%, 30.3%, and 19.42%, which were consistent with the volatile and fixed carbon contents ($V_{ad} + FC_{ad}$). The calculated combustion performance indices (S_n) of CG for the three samples were 6.01×10^{-10}, 29.42×10^{-10}, and 15.65×10^{-10} %^{2}/(min^2 K^3). The S_n values increased with an augment of $V_{ad} + FC_{ad}/A_{ad}$. Sample 2 had a higher de-volatilization rate, burnout performance, and total mass loss, and it was easier to ignite during the spontaneous combustion process. The combustion performance of CG was more favorable when $V_{ad} + FC_{ad}$ was high and the ash content was low. In addition, the CG samples from the same mine area contained analogous hydroxyl, aliphatic, and oxygen functional groups, and aromatic compounds.

1. Introduction

Coal gangue (CG) is a mixture of organic and inorganic compounds and mineral materials [1], that are fused together with coal deposits during the coal formation process [2]. CG is a complex industrial solid waste generated from the coal mining and washing process [3]. Because of long-term stacking, spontaneous combustion frequently occurs in coal and carbonaceous materials [4]; this phenomenon has been reported worldwide [1,2,4–6].

Spontaneous ignition of gangue hills has generated numerous environmental and ecological hazards, such as toxic and harmful gas emissions that pollute the air [7] and heavy metal ions that contaminate the soil and water [8]. Moreover, toxic substances generated from CG hills, such as mercury, have threatened the health of people residing around and working in the mining industry zone [9]. In addition, the waste dump may lead to fire or explosion and cause casualties [6,10].

Coal production in China was 3.68 billion tons in 2015 [11], accounting for 47% of the global share. The discharge rate of CG reached approximately 10–15% of raw coal production [9], equivalent to 368–552 million tons. The total inventory of CG in China is estimated to be approximately 4.5–5.0 Gt [12], with an annual increase of 0.37–0.55 Gt [13]. Large amounts of waste are stacked to form a huge waste dump, which occupy large areas and are potentially hazardous [14–16]. More than 1600 CG hills are present in China, and over 300 of these hills have exhibited spontaneous combustion with smoke produced during the day and night. The western and northern regions of China are major coal-producing

* Corresponding author.
E-mail address: shucm@yuntech.edu.tw (C.-M. Shu).

http://dx.doi.org/10.1016/j.applthermaleng.2017.01.083
1359-4311/

Nomenclature

DTG_{max}	maximum combustion rates (%/min)
t_p	corresponding time of DTG_{max} (min)
t_i	ignition time (min)
$\Delta t_{1/2}$	time range of $DTG/DTG_{max} = 0.5$ (min)
t_h	burnout time (min)
$(dw/d\tau)_{max}$	maximum rate of oxidation reaction at the peak (%/min)
$(dw/d\tau)_{ave}$	average rate of CG obtained by DTG area integration (%/min)
D_i	ignition index
D_h	burnout index
S_n	comprehensive combustion performance index
T_1	characteristic temperature of maximum evaporation of water and desorption of gases (°C)
T_2	characteristic temperature of maximum oxidization mass gain (°C)
T_3	characteristic temperature of ignition point (°C)
T_4	characteristic temperature of maximum mass loss rate (°C)
T_5	characteristic temperature of burnout point (°C)

areas, and the spontaneous ignition of CG hills in these areas has caused severe pollution [7,9].

Because of the growing public appeals for environmental protection, local governments and mining companies have made concerted efforts to govern spontaneous combustion of the CG hills. For example, in Wuhai, a city located in western Inner Mongolia, China and famous for its Wuda coalfield, which is a global hot spot for coal fire research, 80 of the total 196 ignition points in refuse discharge fields were extinguished by June 2016. Furthermore, of the entire fire area of 1.25 million m^2, the fire management project processing reached 539,200 m^2. Although the fire control project was extremely expensive and time consuming, considerable efforts were made to extinguish 53 ignition points in the 199,300 m^2 area [17].

Several investigations have been conducted to elucidate the mechanisms underlying the spontaneous combustion of CG. Zhang et al. investigated the combustion behaviors and thermokinetic parameters of 11 CGs using thermogravimetry (TG) to evaluate the effects of feedstock properties [18]. Furthermore, Urbański and Walker have reported that the self-ignition spot is 1.5–2.0 m below the surface [19,20]. The phenomenon of spontaneous combustion during the initial stage occurs at 60–80 °C with organic and oxidized mineral materials [21]. Zhou et al. investigated thermal and trace-element partitioning behaviors during the cocombustion of biomass with CG [8,15]. In addition, Wang et al. reported five characteristic temperatures of six types of coal ranks at different oxidation stages [22]. Niu et al. examined the changes of the functional groups of Xundian coal using in-situ Fourier transform infrared (FTIR) spectroscopy [23]. Ran et al. examined the combustion and pyrolysis kinetic characteristics of CG under different conditions [24]. The coal-oxygen recombination theory has been accepted by numerous researchers [2]. According to this theory, a CG hill consists of a discontinuous porous medium. The oxygen penetrates into surface cracks, resulting in oxidation reaction with some active groups of gangue, and the heat generated in the oxidation process causes spontaneous combustion. However, ignition of a CG hill is a complex combustion system driven by internal and external factors. A uniform viewpoint on the mechanism underlying the spontaneous combustion of CG is not yet available.

In this study, we used simultaneous TG-FTIR spectroscopy to investigate TG, derivative thermogravimetry (DTG), FTIR, characteristic temperatures, and functional groups during the oxidation process of CG under air atmosphere. The study of CG and its oxidation characteristics is crucial for evaluating the relationship between the macroscopic properties of spontaneous combustion and the microstructure characterization of CG. Simultaneously, this study also provided an appropriate method for revealing the spontaneous chemical reaction and mechanism of CG in its spontaneous combustion process. Finally, this study offers evidence that can be applicable in the control engineering of self-heated colliery spoil heaps in China.

2. Experimental and methods

2.1. Sample preparation

CG samples were collected from the Gongwusu coal mine, located in Wuhai City, Inner Mongolia, China (Fig. 1). Fresh test samples were packed in bags and taken to the laboratory. Particles with a size between 80 and 120 mesh (0.125–0.180 mm) were sieved after pulverization. The selected gangue particles were then transferred into the reaction bed for testing under air atmosphere.

2.2. Proximate analysis

We determined the moisture, ash, volatile, and fixed carbon contents using the 5E-MAG6700 proximate analyzer (Qiulong Instruments, Changsha City, Hunan Province, China) according to the National Standards of China GB/T212-2008, which is equivalent to the American Standards of ASTM-D5142-2009.

2.3. TG-FTIR spectroscopy

The characteristic parameters of distinct oxidation stages of CG, such as the mass loss, mass loss rate, and characteristic temperature, were screened and tested through TG (Pyris 1 TG, PerkinElmer, Fremont, California, USA). Moreover, the related data of the functional groups of released gases in the heating process were scanned through FTIR spectroscopy (Spectrum 100, PerkinElmer, Fremont, California, USA), with a scanning range was from 4000 to 650 cm^{-1}. In addition, IR spectral peaks were analyzed using PeakFit® (Version 4.12). The method of second derivative minima was then used to detect hidden peaks in the spectra, and the peak type was reconstructed using the Lorentz–Gauss (amplitude) equation. The air flow rate was 20 mL/min and the heating rate was 20 °C/min from 30 to 900 °C.

2.4. Combustion performance method

The ignition index (D_i) and burnout index (D_h) are described in Eqs. (1) and (2), respectively [17]. In view of the applications, D_i and D_h can indicate the ignition and burnout performance of CG, respectively:

$$D_i = \frac{DTG_{max}}{t_p \cdot t_i} \quad (1)$$

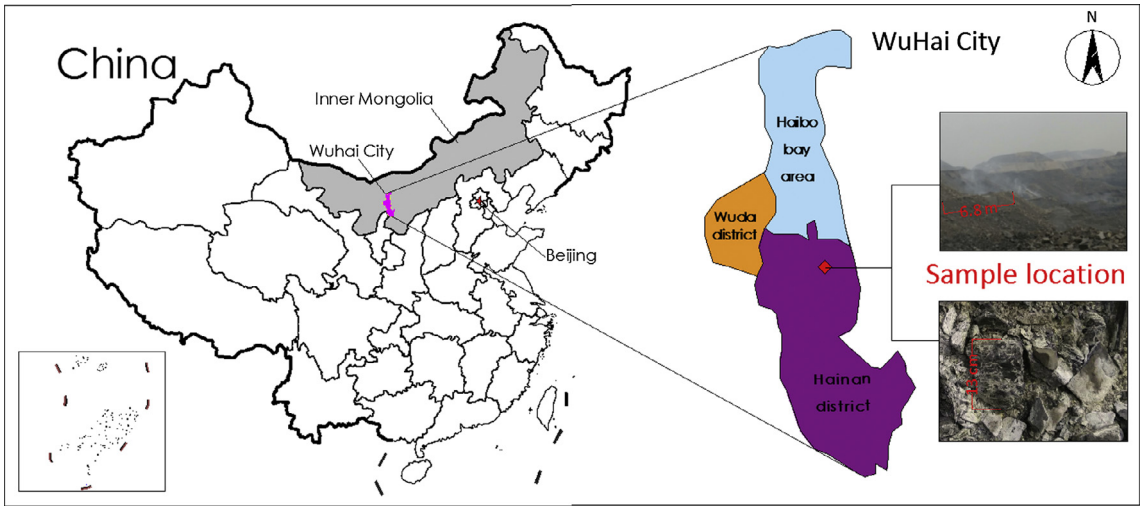

Fig. 1. Geographical localization of the Gongwusu coal mine in Wuhai City, Inner Mongolia, China.

$$D_h = \frac{DTG_{max}}{\Delta t_{1/2} t_p \cdot t_h} \quad (2)$$

where DTG_{max} is the maximum combustion rate, t_p represents the corresponding time of DTG_{max}, t_i is the ignition time, $\Delta t_{1/2}$ is the time range of $DTG/DTG_{max} = 0.5$, and t_h is the burnout time.

The comprehensive combustion performance index (S_n) can be used to evaluate the ignition, combustion, and burnout properties of CG [18,24]. Generally, samples with a high S_n value have a more satisfactory combustion performance [25]. On the basis of the TG and DTG profiles, S_n is described in Eq. (3) as follows:

$$S_n = \frac{(dw/d\tau)_{max} \cdot (dw/d\tau)_{ave}}{T_3^2 \cdot T_5} \quad (3)$$

where $(dw/d\tau)_{max}$ is the maximum rate of oxidation reaction at the peak (%/min), and $(dw/d\tau)_{ave}$ is the average rate of CG obtained through integration of the DTG area (%/min).

3. Results and discussion

3.1. Proximate analysis

The results of the proximate analysis of CG are listed in Table 1. Generally, moisture in CG is present as free and combined water, and high amounts can affect the stability and thermal conductivity of spontaneous combustion [24]. The moisture contents of Samples 1–3 were 2.90%, 2.08%, and 1.22%, respectively. Notably, the ash is the main component of CG, and the highest ash content was found in Sample 1 (83.03%). The volatile contents of the samples were 12.38%, 15.61%, and 11.08%. In addition, substantial differences were identified between the fixed carbon contents of the samples, which were 1.70%, 13.76%, and 8.69%. The main mineral phases of CG include quartz, kaolinite, illite, calcite, and pyrite [18].

3.2. TG/DTG results

The TG and DTG curves of the samples during the oxidation process are presented in Figs. 2–4. On the basis of previous studies [22,26], five characteristic temperatures were defined in the oxidation reaction process of CG. T_1, T_2, T_3, T_4, and T_5 represented the temperatures of the maximum evaporation of water and desorption of gases, maximum oxidization mass gain, ignition point, maximum mass loss rate, and burnout point, respectively. Detailed information regarding the oxidation and combustion characteristic parameters of the samples is listed in Table 2.

The T_2 values of the three samples ranged from 267.6 to 244.3 °C. Notably, the T_2 value of Sample 1 was higher than those of Samples 2 and 3, and the T_2 value was consistent with the ash content. An high ash content can affect oxygen diffusion and heat transfer [28], and it may have inhibited the oxidation rate of Sample 1. Thus, this sample reached its T_2 quite late. The T_3 values of the Samples 1–3 were 457.5, 454.4, and 444.3 °C, respectively; similarly, the T_4 values were 520.4, 518.8, and 511.7 °C, respectively. Thus, both the T_3 and T_4 values indicated a declining trend. In addition, the T_5 values ranged from 710.4 to 742.4 °C. Wang et al. indicated that a high volatile content may increase the oxidation rate, and the characteristic temperatures may be reached early [22]. Nevertheless, the characteristic temperatures of CG did not always change in accordance with the volatile and ash contents. Other factors, such as the fixed carbon content and oxygen adsorption, can also affect the characteristic temperature point and oxidation process of CG [18]. We calculated the ignition and burnout performance in this study to analyze the combustion performance of CG.

According to the variation of TG curves, the spontaneous combustion process of CG was divided into four phases [26]: Water evaporation and gas desorption, oxygen-absorption mass gain, decomposition and combustion mass loss, and residue. These phases were marked as I, II, III, and IV, respectively. The mass losses

Table 1
Proximate analysis of the CG collected from the Haibowan coalfield.

Sample	M_{ad} (%)	A_{ad} (%)	V_{ad} (%)	FC_{ad} (%)	S (%)
No. 1	2.90	83.03	12.38	1.70	2.94
No. 2	2.08	68.88	15.61	13.76	4.90
No. 3	1.22	79.15	11.08	8.69	2.67

Notes: ad, air dry basis; M, moisture; A, ash yield; V, volatile matters; FC, fixed carbon; S, total sulfur.

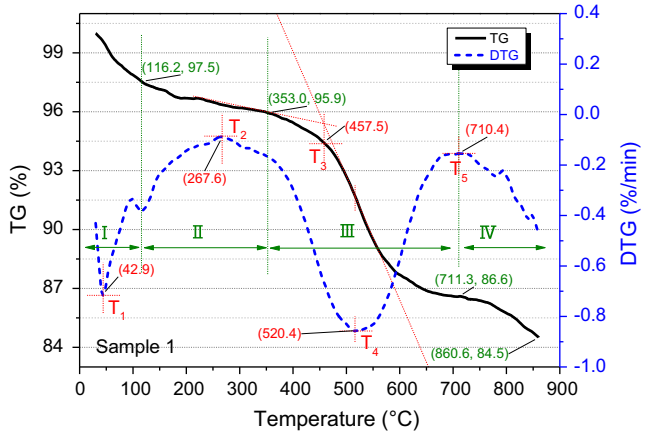

Fig. 2. TG and DTG curves of Sample 1 in the oxidized process at a heating rate of 20 °C/min.

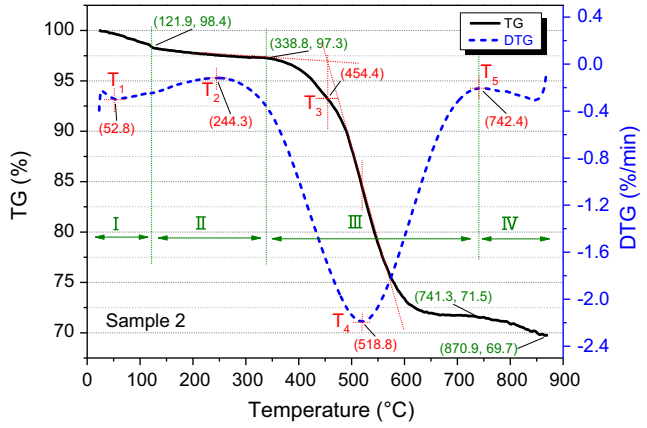

Fig. 3. TG and DTG curves of Sample 2 in the oxidized process at a heating rate of 20 °C/min.

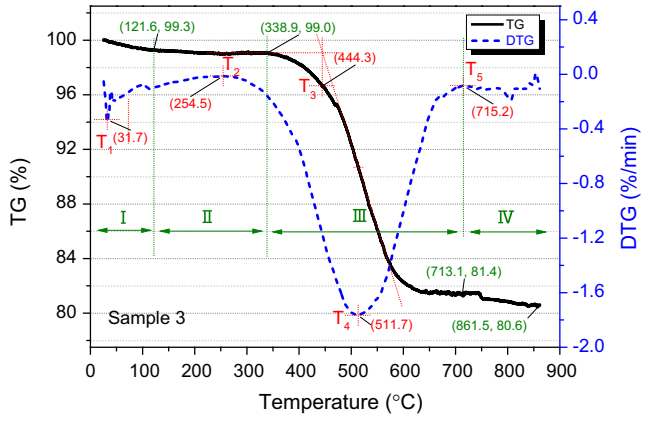

Fig. 4. TG and DTG curves of Sample 3 in the oxidized process at a heating rate of 20 °C/min.

that occurred in each phase are listed in Table 2. With an increase in temperature, the samples each had a low mass loss in the initial stage and then high mass loss until burnout. The mass loss in the phases I, II, III, and IV ranged from 0.72% to 2.45%, 0.20% to 1.61%, 9.35% to 25.75%, and 0.80% to 2.13%, respectively. In all the samples, the highest mass loss occurred during phase III, which may be related to volatile and fixed carbon contents [27]. Generally, the higher the volatile content of CG, the higher the devolatilization rate of volatile pyrolysis and total mass loss at the end of the oxidation process [29]. The total mass loss of the three samples was 15.50%, 30.30%, and 19.42%, respectively, a finding that is consistent with those reported in previous studies [22,24].

Table 2
Spontaneous combustion characteristic parameters of the CG.

Sample	No. 1	No. 2	No. 3
T_1 (°C)	42.9	52.8	31.7
T_2 (°C)	267.6	244.3	254.5
T_3 (°C)	457.5	454.4	444.3
T_4 (°C)	520.4	518.8	511.7
T_5 (°C)	710.4	742.4	715.2
I mass loss (%)	2.45	1.62	0.72
II mass loss (%)	1.61	1.10	0.23
III mass loss (%)	9.35	25.75	17.67
IV mass loss (%)	2.10	1.83	0.80
Total mass loss (%)	15.50	30.30	19.42

3.3. Calculation of combustion characteristic parameters of CG

We calculated S_n, D_i, and D_h to delve into the oxidation characteristics of the samples; the index values are listed in Table 3. The low calorific value of CG [30] is based on low volatile and fixed carbon contents, and the high ash contents. Therefore, CG is unsuitable for use as a fuel. As summarized in Table 3, the maximum oxidation reaction rates of Samples 1–3 at their peaks were −0.86, −2.18, and −1.77 °C/min, respectively. Thus, Sample 2 had the highest oxidation reaction rate at its peak. Moreover, the volatile and fixed carbon contents of Sample 2 were higher than those of Samples 1 and 3 (Table 1), indicating that Sample 2 had the maximum volatile release rate at its peak temperature of 518.8 °C.

The relationships between the combustion characteristic parameters (D_i, D_h, and S_n) and $V_{ad} + FC_{ad}/A_{ad}$ are illustrated in Figs. 5 and 6. Fig. 5 revealed that the calculated index S_n had a high linearity fitting performance with $V_{ad} + FC_{ad}/A_{ad}$ (correlation coefficient, $R = 0.975$), which indicated the feasibility and validity of this method. S_n increased with an increase in $V_{ad} + FC_{ad}/A_{ad}$. The S_n value of Sample 2 ($29.42 \times 10^{-10}\%^2/\text{min}^2\ \text{K}^3$) was higher than those of Samples 1 and 3 were, indicating that the combustion characteristics of Sample 2 were more favorable than those of Samples 1 and 3 were.

The results of the ignition index D_i and burnout index D_h were also in accordance with the results for S_n (Fig. 6). The D_i and D_h values indicated that Sample 2 had more satisfactory ignition and burnout characteristics than the other samples did. Additionally, the combustion characteristic parameters indicated that, compared with Samples 1 and 3. Sample 2 had a higher devolatilization rate, burnout performance, and total mass loss, and was easier to ignite. The volatile, fixed carbon, and ash contents of CG have crucial roles in the oxidation process. Herein, the combustion performance of CG was more satisfactory when the volatile and fixed carbon contents were high and the ash content was low, which is consistent with the results reported in previous studies on coal [18,24,30].

3.4. FTIR spectroscopy

To further investigate the reaction mechanism of CG during its spontaneous combustion, in-situ FTIR was used to examine the functional group variation of CG with various temperatures under air atmosphere. Studies have reported that aromatic, aliphatic, and oxygen functional groups are the three main organic compounds involved in CG decomposition [31]. Moreover, peaks appearing in

Table 3
Combustion parameters of the different samples.

Sample	$(dw/d\tau)_{max}$ (%/min)	$(dw/d\tau)_{ave}$ (%/min)	$D_i \times 10^4$	$D_h \times 10^4$	$S_n \times 10^{10}$ (%^{2}/(min^2 K^3))
No. 1	−0.86	−0.36	−15.07	−0.44	6.01
No. 2	−2.18	−0.70	−40.54	−2.14	29.42
No. 3	−1.77	−0.45	−30.16	−1.89	15.65

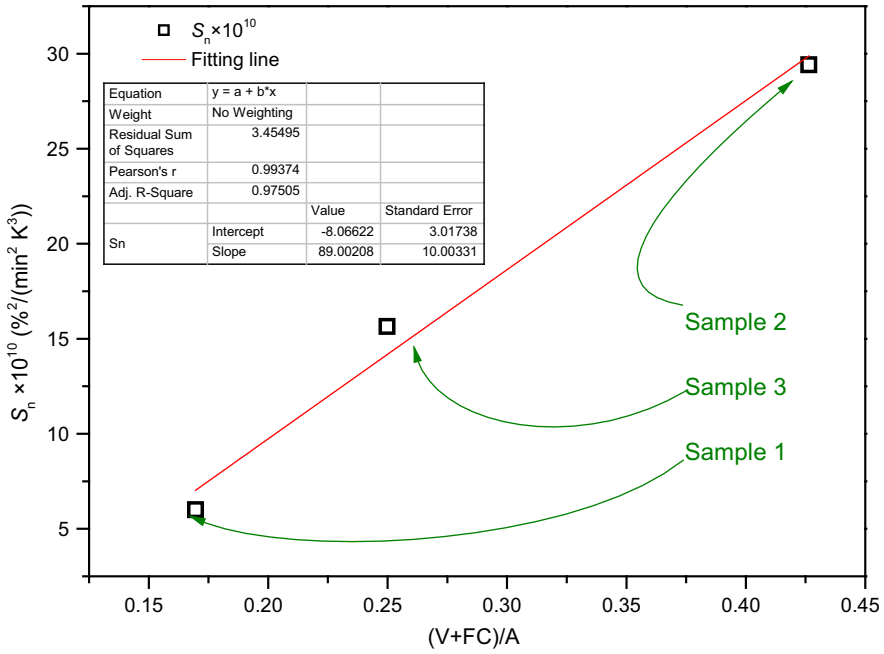

Fig. 5. Relationship between S_n and $(V_{ad} + FC_{ad})/A_{ad}$.

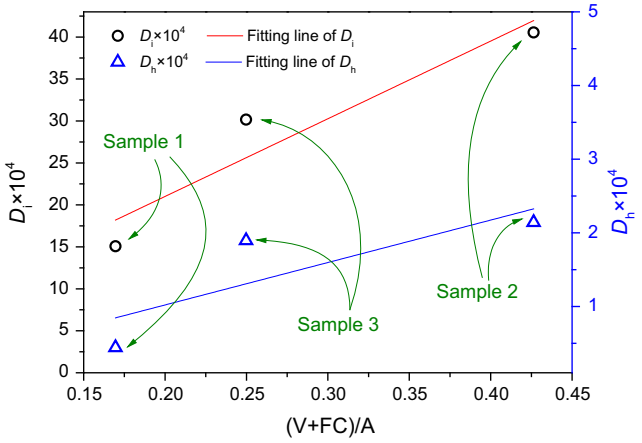

Fig. 6. Relationships between D_i, D_h, and $(V_{ad} + FC_{ad})/A_{ad}$.

the ranges from 3600 to 3000, 3000 to 2700, 1800 to 1000, and 900 to 700 cm^{-1} were the critical spectral ranges in the investigation of organic compounds in CG [32]. The FTIR spectra of the CG in this study at diverse temperatures are illustrated in Fig. 7.

Fig. 7 shows that the spectrum structure of each sample was similar at various heating stages. However, a difference was observed in their peak heights and areas. The number of functional CG groups changed with an increase in heating. The professional software PeakFit® was used to reconstruct and analyze the spectral data with correlation coefficient $R^2 > 0.99$. The functional groups of CG obtained at a temperature of 50 °C are depicted in Fig. 8 and outlined in Table 4.

According to the FTIR spectra in Fig. 8 and Table 4, the spectrum number and waveform morphology of the three samples were consistent at a temperature of 50 °C, indicating that these samples contained analogous hydroxyl, aliphatic, and functional groups, as well as aromatic compounds. This finding could be attributable to the collection of the samples from the same colliery region; thus, the geological environment and coal age of the samples were similar.

According to previous studies [34–36], the FTIR spectra ranging from 4000 to 3500 cm^{-1} have an O—H stretching vibration under dissociated conditions [22]; the wave number ranging from 1900 to 1300 cm^{-1} verified the O—H stretching vibration of an in-of-plane ring bend. The absorbance bands of water in the three samples might be attributable to the dehydration of crystalline minerals ($Al_2O_3{\cdot}2SiO_2{\cdot}2H_2O$) in CG by losing both free water (approximately 1654 cm^{-1}) and chemically bonded water (approximately 3740 cm^{-1}) [35].

The wave number ranging from 3100 to 3000 cm^{-1} belongs to an adjacent double bond or aromatic ring, indicating C—H stretching [33]. Furthermore, the peaks in the range from 2240 to 2060 cm^{-1} were considered to have C—O stretching [22]. The integral areas of CO and CO_2 stretching vibrations at 400–500 °C were more evident than those at other heating stages, indicating that the gas production was very high in this stage. The regular integral areas of CO and CO_2 stretching vibrations were consistent with the fastest reaction stage in DTG curves (Figs. 2–4).

The main oxidation products of CG at 50 °C were broad-peak transalkanes (—CH_3) that were widely distributed at approximately 2945 cm^{-1}, C—C bonds in aromatics rings in the region between 1500 and 1400 cm^{-1}, and C—O stretching vibrations in the region between 1320 and 1000 cm^{-1} that corresponded to

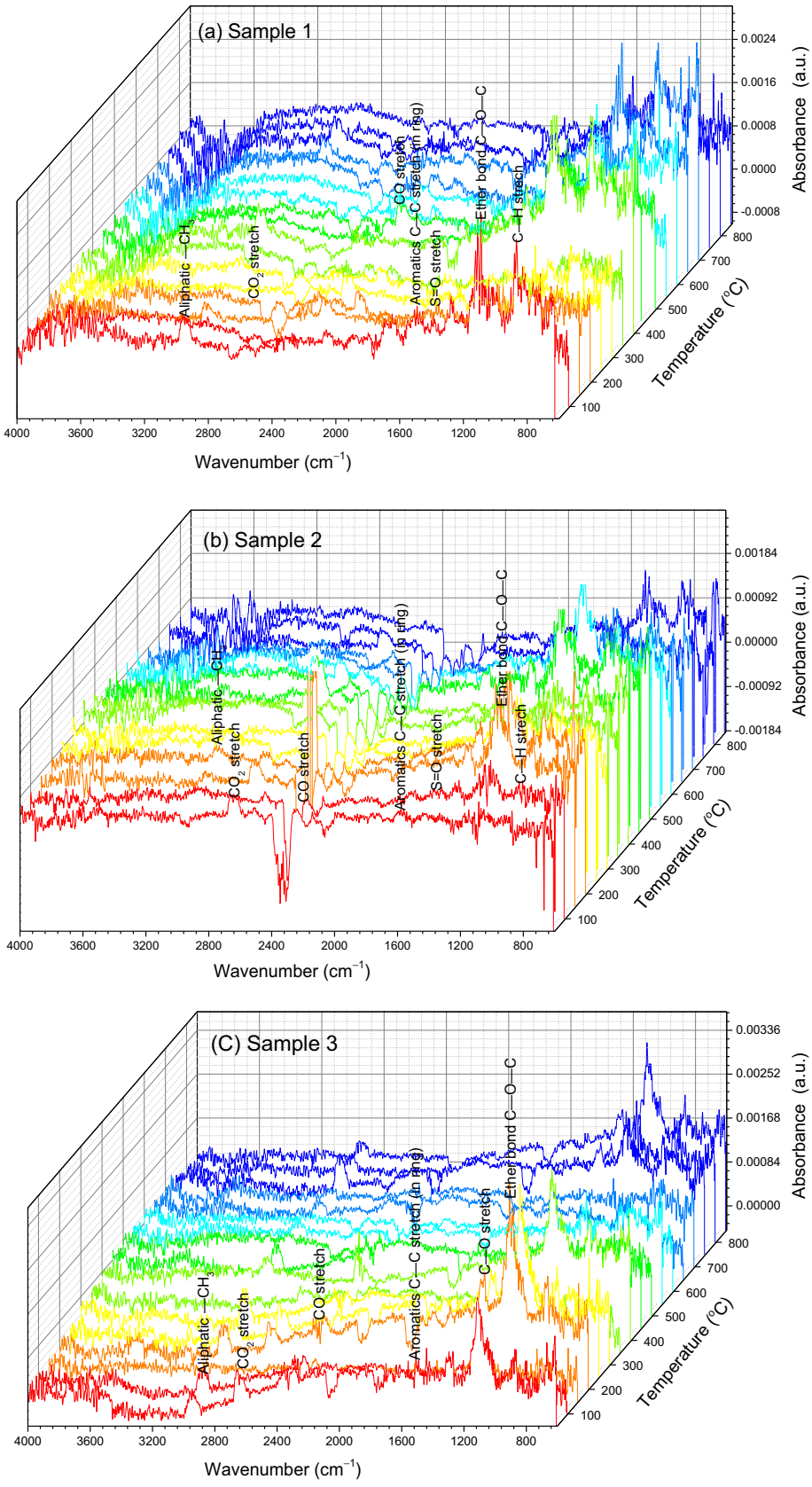

Fig. 7. FTIR spectra of the CG. (a) Sample 1; (b) Sample 2; and (c) Sample 3.

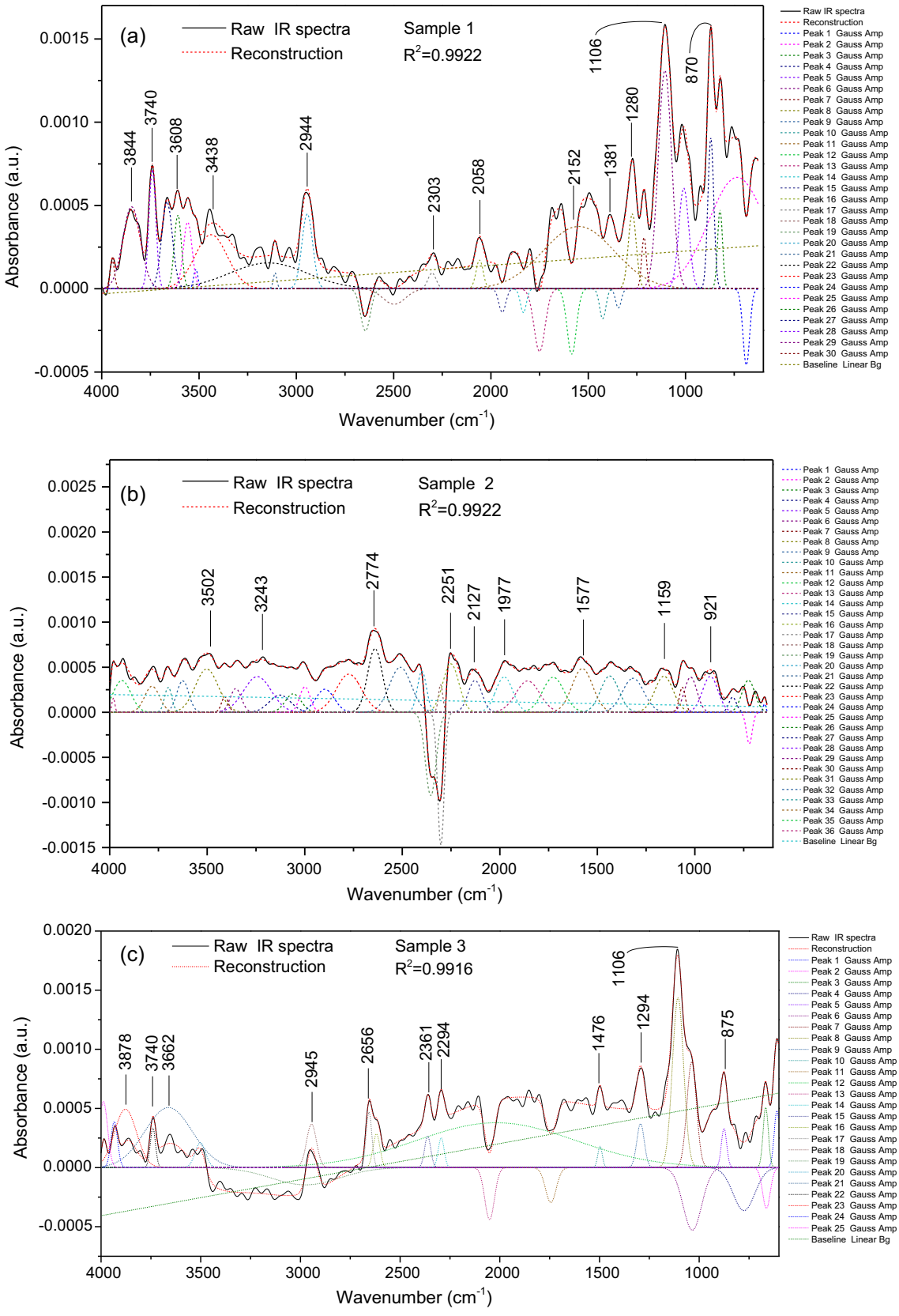

Fig. 8. FTIR spectra of the samples in the oxidized process at 50 °C. (a) Sample 1; (b) Sample 2; and (c) Sample 3.

Table 4
Analysis of the absorption peaks of Samples 1–3 at 50 °C.

Group and class	Band stretch (cm^{-1})	Wavenumber peak (cm^{-1})
Hydroxy	4000–3700, O—H stretch, Free OH groups [37]	3878, 3844, 3740
	3700–3200, O—H stretch, H-bonded, alcohols, phenols, crystalliferous water of crystalline minerals	3662, 3608, 3502, 3438
	3100–3000, C—H stretch, aromatics, adjacent to a double bond or aromatic ring [33]	3050
Aliphatic	3000–2850, C—H stretch, alkanes, $-CH_3$	2945
	2650–2200, CO_2 stretching vibration [22]	2361
	2200–1900, CO stretching vibration [22]	2051, 2058
Functional groups and aromatic	1800–1600, C=O stretching vibration	1654, 1549
	1500–1400, C—C stretch (in-ring), aromatics	1500, 1497, 1476
	1420–1300, S=O stretching vibration, sulfur-oxygen compounds, sulfones, sulfoxides, etc. [33]	1380, 1345
	1320–1000, C—O stretching vibration, alcohols, carboxylic acids, esters, ethers	1294, 1281, 1294, 1159, 1106
	1037, Si—O—Si stretch, Si—O in quartz [34]	
Aromatics in low wave region and ash matter	C—H stretching vibration	875, 870, 746, 735

alcohols, carboxylic acids, esters, and ethers [34]. The C—O stretching vibrations at approximately 1106 cm^{-1} were evident at temperatures between 300 and 400 °C, indicating that the oxidation activity of CG started to strengthen from this stage.

The peaks of aromatic compounds in the low wave region and ash matter C—H stretching vibrations were observed at approximately 870 cm^{-1}, whereas aromatic rings and unsaturated aliphatic hydrocarbons were observed at approximately 746 cm^{-1}. Concurrently, the mineral peak of crystalliferous water for the crystalline minerals quartz and kaolinite appeared in the CG spectra. S=O stretching vibrations were observed between 1420 and 1300 cm^{-1}; these vibrations corresponded to sulfur-oxygen compounds, sulfones, and sulphoxides [34,36]. Furthermore, SO_2 was detected at approximately 1380 cm^{-1} in Sample 1 and at 1345 cm^{-1} in Sample 2. In the course of the CG oxidation process, the peak amplitude of the S=O of Sample 2 was evidently higher than those of Samples 1 and 3 were at the same temperature. Therefore, Sample 2 had relatively stronger S=O stretching vibrations, and its sulfur content (Table 1) may have released more SO_2 products.

3.5. Implications for preventing the spontaneous combustion of CG

Understanding the spontaneous combustion characteristics of CG is the foundation for the selection of an appropriate fire control method. This study revealed the following regarding the CG fire hazard control project of Haibowan coalfield, Wuhai.

Basic information about CG was obtained through proximate and elemental analyses. Generally, heating spots were artificially divided into three areas according to their temperature or depth: The cooling zone, oxidation zone, and suffocation zone [38]. The high-temperature region (oxidation zone) ranged from 2 to 4 m [39], and the depth of the burning layer of CG (oxidation zone) was between 1.5 and 2.5 m [1]. The five characteristic temperatures determined using TG curves were significant, and they predicted the high-temperature areas. Taking economic and technical feasibility into consideration, an appropriate treatment method could be selected for various CG partition areas, such as the digging method, firefighting gel injection [40], or CO_2 injection [41] for the burning area (temperature > 450 °C). Conversely, the water sprinkler method, and cooling by heat pipe [42] can be used for the oxidation area (temperature 100–450 °C). Furthermore, a noncombustible material can cover the remaining areas (temperature < 100 °C).

The performances of the ignition, burnout, and comprehensive combustion for Haibowan CG are indicated by the combustion characteristic parameters, which also provided basic information for determining the treatment process. For example, locating CG with a high volatile content, fixed carbon content, and comprehensive index should be a priority, whereas the location of CG with low performance characteristics can be conducted relatively late because of its high ignition point and longer ignition time. The functional group confirmed by the FTIR spectra of Haibowan CG can be used to select a relevant inhibitor or a blocking agent. However, to prevent the spontaneous combustion of CG, the selected paralyzant can be used to increase the apparent activation energy by spraying it on the surface of colliery waste piles, or ionic liquids can be used to fracture the chemical bonds of CG [43].

The spontaneous combustion characteristics of CG hills play a crucial role in the selection of a suitable treatment method that can efficiently improve the accuracy and economy of a fire extinguishing project.

4. Conclusions

(a) According to the TG/DTG curves, mass loss occurred during the heating process in the four phases, and the total mass loss of the Samples 1–3 were 15.5%, 30.3%, and 19.42%, respectively. The five characteristic temperatures ranged from 31.7 to 52.8 °C, 244.3 to 267.6 °C, 444.3 to 457.5 °C, 511.7 to 520.4 °C, and 710.4 to 742.4 °C, respectively.

(b) The comparison of the combustion characteristic parameters of the samples collected from different parts revealed that compared with Samples 1 and 3, Sample 2 had satisfactory ignition and burnout performance and a higher devolatilization rate. The combustion performance of CG was improved when the volatile and fixed carbon contents were high and the ash contents was low.

(c) Scanning the spectra revealed that the samples contained analogous hydroxyl, aliphatic, and functional groups, as well as aromatic compounds. The characteristic peaks identified in the current study were CH_4 (approximately 2944 cm^{-1}), CO_2 (approximately 2361 cm^{-1}), CO (approximately 2051 cm^{-1}), and H_2O (approximately 3740 and 1654 cm^{-1}). The spectra data also indicated that the C—O stretching vibration was evident at temperatures between 300 and 400 °C, and CO and CO_2 vibrations increased at temperatures between 400 and 500 °C.

Acknowledgments

The study was sponsored by the National Natural Science Foundation of China (Nos. 51504186, 51504187, and 51574193). We are grateful to X.B. Li, H.F. Lu, and F.M. Ye for their helpful data processing suggestions and experimental support. Special thanks are given to our engineer B.Y. Wang for his support in CG collection.

References

[1] M.J. Fabiańska, J. Ciesielczuk, Ł. Kruszewski, M. Misz-Kennan, D.R. Blake, G. Stracher, Gaseous compounds and efflorescences generated in self-heating coal-waste dumps – a case study from the Upper and Lower Silesian Coal Basins (Poland), Int. J. Coal Geol. 117 (2013) 247–261.

[2] G.B. Stracher, Coal and peat fires: a global perspective: Volume 1: Coal-geology and combustion, Int. J. Digit Earth 5 (2012) 458–469.

[3] Z. Cao, Y. Cao, H. Dong, J. Zhang, C. Sun, Effect of calcination condition on the microstructure and pozzolanic activity of calcined coal gangue, Int. J. Miner. Process. 146 (2016) 23–28.

[4] J. Ribeiro, E. Ferreira da Silva, D. Flores, Burning of coal waste piles from Douro coalfield (Portugal): petrological, geochemical and mineralogical characterization, Int. J. Coal Geol. 81 (2010) 359–372.

[5] A. Prakash, R. Gupta, A. Saraf, A Landsat TM based comparative study of surface and subsurface fires in the Jharia coalfield, India, Int. J. Remote Sens. 18 (1997) 2463–2469.

[6] G. Fan, D. Zhang, X. Wang, Reduction and utilization of coal mine waste rock in China: a case study in Tiefa coalfield, Resour. Conserv. Recy. 83 (2014) 24–33.

[7] X. Querol, M. Izquierdo, E. Monfort, Environmental characterization of burnt coal gangue banks at Yangquan, Shanxi Province, China, Int. J. Coal Geol. 75 (2008) 93–104.

[8] C. Zhou, G. Liu, T. Fang, Partitioning and transformation behavior of toxic elements during circulated fluidized bed combustion of coal gangue, Fuel 135 (2014) 1–8.

[9] Y. Liang, H. Liang, S. Zhu, Mercury emission from spontaneously ignited coal gangue hill in Wuda coalfield, Inner Mongolia, China, Fuel 182 (2016) 525–530.

[10] Y. Xing, Z. Zhang, Y. Pan, Discussion on reasons and comprehensive control of spontaneous combustion and explosion of gangue of Tian'an coal mining group, Henan Sci. 26 (2008) 712–722.

[11] S. David, UPDATE 1−China 2015 Coal Output Drops 3.5 pct on Soft Demand, Pollution Curbs. Reuters Mon Jan 18, 2016. <http://www.reuters.com/article/china-economy-output-coal-idUSL3N1531CD>.

[12] M. Li, Ecological restoration of mineland with particular reference to the metalliferous mine wasteland in China: a review of research and practice, Sci. Total Environ. 357 (2006) 38–53.

[13] B. Liang, L. Xiao, Mechanism and Numerical Prediction of Coal Gangue Leachate to Groundwater Pollution, Liaoning Science and Technology Publishing House, Changchun, China, 2012.

[14] W. Li, L. Chen, T. Zhou, Q. Tang, T. Zhang, Impact of coal gangue on the level of main trace elements in the shallow groundwater of a mine reclamation area, Min. Sci. Technol. 21 (2011) 715–719.

[15] C. Zhou, G. Liu, D. Wu, T. Fang, R. Wang, F. Xiang, Mobility behavior and environmental implications of trace elements associated with coal gangue: a case study at the Huainan Coalfield in China, Chemosphere 95 (2014) 193–199.

[16] H.M. Liu, C.B. Wang, Y. Zhang, X.Z. Huang, Y.C. Guo, J.W. Wang, Experimental and modeling study on the volatilization of arsenic during co-combustion of high arsenic lignite blends, Appl. Therm. Eng. 108 (2016) 1336–1343.

[17] G. Yan, X. Zhao, Wuhai makes its Great Efforts to Carry out Mining Comprehensive Environmental Action, En.northnews.cn. <http://www.northnews.cn/2016/0602/2188324.shtml>.

[18] Y. Zhang, Y. Guo, F. Chen, Investigation of combustion characteristics and kinetics of coal gangue with different feedstock properties by thermogravimetric analysis, Thermochim. Acta 614 (2015) 137–148.

[19] J. Urbański, Technical Re-cultivation of Mine Waste Dumps with Particular Reference to Fire Protection. Training Materials, The Association of Mining Engineers and Technics, Katowice, Poland, 1983 (in Polish).

[20] S. Walker, Uncontrolled Fires in Coal and Coal Wastes, IEA Coal Research, London, 1999. ((CCC/16) ISBN 92-9029-3247-1).

[21] E.V. Sokol, High-temperature processes of organic fuel decomposition as a thermal source for pyrometamorphic transformations, in: G.G. Lepezin (Ed.), Combustion Metamorphism, Publishing House of the Siberian Branch of Russian Academy of Sciences, Novosybirsk, Russian, 2005, pp. 22–31.

[22] C. Wang, Y. Yang, Y. Tsai, Spontaneous combustion in six types of coal by using the simultaneous thermal analysis – Fourier transform infrared spectroscopy technique, J. Therm. Anal. Calorim. (2016) 1–12.

[23] Z.Y. Niu, G.J. Liu, H. Yin, C.C. Zhou, D. Wu, B. Yousaf, C.M. Wang, In-situ FTIR study of reaction mechanism and chemical kinetics of a Xundian lignite during non-isothermal low temperature pyrolysis, Energy Convers. Manage. 124 (2016) 180–188.

[24] J. Ran, B. Niu, L. Zhang, Study on general combustion performance and kinetic characteristics of combustion of coal residue, Proc. CSEE 26 (2006) 58–62 (in Chinese).

[25] L. Ge, Y. Zhang, C. Xu, Z. Wang, J. Zhou, K. Cen, Influence of the hydrothermal dewatering on the combustion characteristics of Chinese low-rank coals, Appl. Therm. Eng. 90 (2015) 174–181.

[26] X. Qi, Q. Li, H. Zhang, H. Xin, Thermodynamic characteristics of coal reaction under low oxygen concentration conditions, J. Energy Inst. (2016) 1–12, http://dx.doi.org/10.1016/j.joei.2016.05.007.

[27] J. Ren, C.J. Xie, X. Guo, Z.F. Qin, J.Y. Lin, Z. Li, Combustion characteristics of coal gangue under an atmosphere of coal mine methane, Energy Fuels 28 (2014) 688–695.

[28] H.M. Wang, C.F. You, Experimental investigation into the spontaneous ignition behavior of upgraded coal products, Energy Fuels 28 (2014) 2267–2271.

[29] M. Wang, X. Ma, Y. Zhang, Study on effect of experimental factor on the pyrolysis of coal gangue, Fly Ash Comprehen. Utiliz. 6 (2011) 37–41.

[30] D. Yu, M. Chen, Y. Wei, S. Niu, F. Xue, An assessment on co−combustion characteristics of Chinese lignite and eucalyptus bark with TG-MS technique, Powder Technol. 294 (2016) 463–471.

[31] O.O. Sonibare, T. Haeger, S.F. Foley, Structural characterization of Nigerian coals by X-ray diffraction, Raman and FTIR spectroscopy, Energy 35 (2012) 5347–5353.

[32] J.V. Ibarra, E. Munoz, R. Mliner, FTIR study of the evolution of coal structure during the coalification process, Org. Geochem. 24 (1996) 725–735.

[33] J. Yan, X. Jiang, X. Han, J. Liu, A TG-FTIR investigation to the catalytic effect of mineral matrix in oil shale on the pyrolysis and combustion of kerogen, Fuel 104 (2013) 307–317.

[34] C. Zhou, G. Liu, S. Cheng, T. Fang, P.K.S. Lams, Thermochemical and trace element behavior of coal gangue, agricultural biomass and their blends during co-combustion, Bioresour. Technol. 166 (2014) 243–251.

[35] Y. Li, Y. Yao, X.M. Liu, H.H. Sun, W. Ni, Improvement on pozzolanic reactivity of coal gangue by integrated, Fuel 109 (2013) 527–533.

[36] G.K. Parshetti, Z. Liu, A. Jain, M.P. Srinivasan, R. Balasubramanian, Hydrothermal carbonization of sewage sludge for energy production with coal, Fuel 111 (2013) 201–210.

[37] G. Xiong, Y. Li, L. Jin, H. Hu, In situ FT-IR spectroscopic studies on thermal decomposition of the weak covalent bonds of brown coal, J. Anal. Appl. Pyrol. 115 (2015) 262–267.

[38] O. Carpentier, D. Defer, E. Antczak, B. Duthoit, The use of infrared thermographic and GPS topographic surveys to monitor spontaneous combustion of coal tips, Appl. Therm. Eng. 25 (2005) 2677–2686.

[39] H. Han, Characteristic and prevention of spontaneous combustion in power plant coal yard, Electr. Power 46 (2013) 98–103 (in Chinese with English abstracts).

[40] J. Deng, Y. Xiao, J. Lu, H. Wen, Y. Jin, Application of composite fly ash gel to extinguish outcrop coal fires in China, Nat. Hazarads 79 (2015) 881–898.

[41] C. Kuenzer, J. Zhang, Y. Sun, Y. Jia, S. Dech, Coal fires revisited: the Wuda coal field in the aftermath of extensive coal fire research and accelerating extinguishing activities, Int. J. Coal Geol. 102 (2012) 75–86.

[42] M. Schmidt, Suhendra, H. Ruter, Heat pipes-suitable for extinguishing underground coal fire? in: Proceedings of Second International Conference on Coal Fire Research, Berlin, Germany, 2010, pp. 433–437.

[43] S. Bhoi, T. Banerjee, K. Mohanty, Beneficiation of Indian coals using Ionic Liquids, Fuel Process. Technol. 151 (2016) 1–10.